

Performance of extended depth of field systems and theoretical diffraction limit

Frédéric Guichard, Frédéric Cao, Imène Tarchouna, Nicolas Bachelard
DxO Labs, 3 Rue Nationale, 92100 Boulogne, France

ABSTRACT

Extended depth of field (EDOF) cameras have recently emerged as a low-cost alternative to autofocus lenses. Different methods, either based on longitudinal chromatic aberrations or wavefront coding have been proposed and have reached the market. The purpose of this article is to study the theoretical performance and limitation of wavefront coding approaches. The idea of these methods is to introduce a phase element making a trade-off between sharpness at the optimal focus position and the variation of the blur spot with respect to the object distance. We will show that there are theoretical bounds to this trade-off: knowing the aperture and the minimal MTF value for a suitable image quality, the pixel pitch imposes the maximal depth of field. We analyze the limitation of the extension of the depth of field for pixel pitch from $1.75\mu\text{m}$ to $1.1\mu\text{m}$, particularly in regards to the increasing influence of diffraction.

Keywords: Extended depth of field, wave front coding, modulation transfer function, diffraction limits.

1. INTRODUCTION

Cameras with Extended Depth of Field (EDOF) have become popular in the camera-phone segment, with several benefits: for instance avoid cost and size of autofocus mechanisms or to enable high resolution wafer level cameras. Roughly speaking, for a “given amount of Modulation Transfer Function (MTF)”, a classical optic concentrates this quantity near the focus (the MTF is large but the DOF is narrow), whereas an EDOF optic diffuses the sharpness all along the optical axis (the DOF is large but the MTF is low). Two concurrent EDOF technologies have emerged these last years. They are both based on a co-optimization of the lens design and an image processing part: longitudinal chromatic aberrations^{15, 16} (LCA) on the one hand and use of wave front coding^{1, 3, 4} (WFC) on the other hand. For the LCA method, the idea is to use a chromatic lens and to sum up the three depths of field associated to the channels R, G and B; its limitations have already been discussed in previous publications^{15, 16}. For the WFC method, the principle is to design the lens so that the MTF is as most insensitive as possible to the (unknown) object distance and easily invertible by digital processing. Many pupils have been designed to implement WFC; they all propose different trade-offs between MTF and DOF. In this paper, we demonstrate that for any symmetric revolution optic there is an absolute trade-off between MTF and DOF. This limit is fixed by diffraction and consequently cannot be overcome. As this limit finds a practical application for symmetric WFC pupil, it will be called the WFC limit.

Our work is organized as follows. In a first step, we model an optical system as an ideal revolution symmetric optic: a stop combined with a phase function and an amplitude function playing the role of the lenses. It therefore corresponds to an optimistic upper bound of what can be achieved optically (by neglecting production loss, sensor effect, etc...).

In a second step, we derive the MTF as a function of the defocus, the phase and amplitude functions. We prove the following result: for any lens revolution symmetric there is an absolute trade-off between MTF and DOF. In other word, whatever the lens (revolution symmetric) with a digital acquisition, knowing the aperture, the f-number, the pixel pitch imposes the maximum attainable DOF. Then, by bounding the WFC limit, we prove that increasing the depth of field (by adequately choosing the phase function) can only be done by a loss in terms of optical MTF. More precisely, we establish a law that quantifies the absolute minimal loss on the MTF through focus for a given targeted extension of the depth of field.

Finally, we use this theoretical analysis to quantitatively estimate possible gains and benefits of the WFC’s approach, in the case of camera phone sensors from $1.75\mu\text{m}$ to $1.1\mu\text{m}$ pixel pitch, and also in the case of higher aperture. In particular, as we know that the WFC’s limit is related to diffraction, we investigate the evolution of these benefits with

the pixel size reduction and the increasing level of diffraction. We conclude with potential evolutions of WFC method that could overcome the discussed limitations.

2. WAVEFRONT CODING MODELING

2.1 Notations

In this paper, we consider revolution-symmetrical optical systems, which are achromatic (of wavelength λ). We use Fresnel's approximation and the study is limited to the optical axis^{7, 8}. We will use the following notations and abbreviations.

- OTF: Optical Transfer Function
- DOF: Depth Of Field
- WFC: Wavefront Coding
- ARSL: Achromatic and revolution symmetric limit (defined in Sect. 3)
- $\vec{\rho} = (\rho, \phi)$: polar coordinates onto the pupil
- $\overline{f(\vec{\rho})}_{Area}$: average value of function $f(\vec{\rho})$ along the domain *Area*
- Ψ : defocus parameter

2.2 Problem positioning

Many optical designs exist in the literature, using a variety of WFC methods. In this paper, we consider an optical system as generally as possible, in order to address all of these methods. The considered optical system is a stop combined to a phase function and an amplitude function. This model could represent a lens, as well as a more complex assembly. Note that this model could be considered as the best case, as it neglects various possible losses (production loss, sensor effects, dispersion due to different system components, etc...)

2.3 Optical set-up

We consider the optical system described in Figure 1. It is composed by a simple pupil. An object (O) placed at the distance d_o from the pupil of diameter L , will be imaged as an image (I) at distance d_i . A light ray emitted by the object O and incident at the image I, passes through the point $M = (\rho, \Phi)$ of the pupil. In order to simplify the notations in the next calculations, the polar coordinates in the pupil are normalized by the lens radius:

$$\vec{\rho} = \left(\frac{\rho'}{L}, \phi \right) = (\rho, \phi) \text{ with } \rho < 1. \quad (1)$$

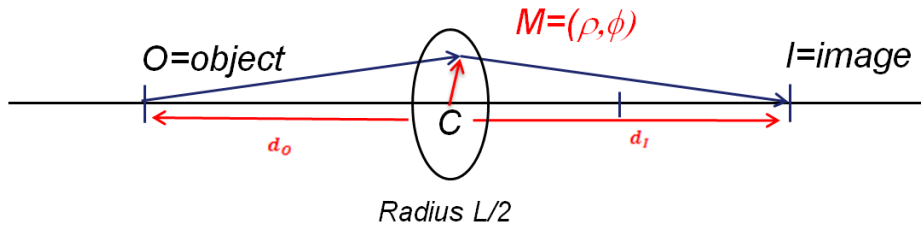


Figure 1 Optical setup: an object O is observed through the optic at a position I

In this paper, we deal with optical systems containing both phase and amplitude modulation. We introduce a complex apodization function in the pupil, expressed as:

$$P(\vec{\rho}) = \begin{cases} |P(\vec{\rho})|e^{j\theta(\vec{\rho})} & \text{if } |\rho| < 1 \\ 0 & \text{else} \end{cases} \quad (2)$$

2.4 Assumptions

For the sake of simplicity, we make the following common assumptions, without affecting the generality of the studied systems. First, all EDOF techniques based on WFC are achromatic. Thus, we will only consider monochromatic signals at a given wavelength λ . Note that this assumption is not valid for EDOF techniques based on LCA. Second, the study is limited to the optical axis. Third, the pupil will be considered as revolution-symmetrical. Thus, we avoid construction artifacts, as well as frequency distortions: P is revolution symmetric, hence only depends on ρ and not on ϕ .

Finally, we use the Fresnel approximation: according to this approximation⁸, a light ray (given by the triplet (OMI) on Fig. 1) entering the lens at radius ρ has a phase delay with respect to the optical axis (ray through OCI on Fig. 1). This phase delay is noted $\Delta_M(\rho)$ and expressed as

$$\Delta_M(\rho) = \frac{\pi L^2}{4\lambda} \left(\frac{1}{d_I} + \frac{1}{d_O} \right) \rho^2. \quad (3)$$

The Fresnel phase delay associated with propagation expressed in (3) can be interpreted as a sum of two terms: the first one is the delay due to the image point position, and the second one is the delay due to the object point position. We study the depth of field in the object plane. The image point will be considered as fixed. The delay associated to the object position is a fundamental parameter. We call it defocus parameter and denote it by

$$\Psi = \frac{\pi L^2}{4\lambda d_O}. \quad (4)$$

Combining (3) and (4), we express the phase delay due to propagation onto the pupil as

$$\Delta_M(\rho) = \frac{\pi L^2}{4\lambda} \frac{1}{d_I} \rho^2 + \Psi \rho^2. \quad (5)$$

2.5 OTF Definition

2.5.1 General Definition

The optical transfer function (OTF) will be expressed in polar coordinates. Let us denote by f_ρ the radial spatial frequency, and f_ϕ the orthoradial one. As the pupil is assumed revolution symmetric, the OTF is revolution symmetric as well, and therefore independent from the orthoradial frequency f_ϕ . To simplify the calculations, we can always assume that $\phi = 0$ and we use the normalized radial frequency u defined by:

$$u = \frac{\lambda f_\rho d_I}{L/2} \quad (6)$$

The normalized frequency vector will be denoted $\vec{u} = (u, 0)$. It has been proved [8] that within the Fresnel approximation, the OTF is equal to the autocorrelation of the pupil.

Considering Figure 2, and denoting $M = \left(\vec{\rho} - \frac{\vec{u}}{2} \right)$ and $M' = \left(\vec{\rho} + \frac{\vec{u}}{2} \right)$, the OTF is equal to the autocorrelation product of (OMI) and (OM'I).

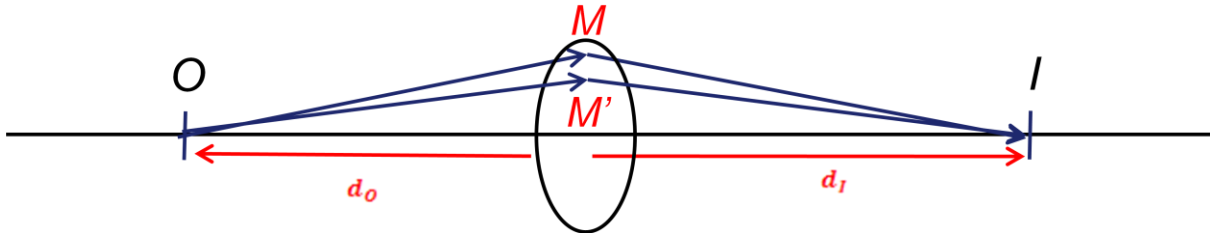


Figure 2 Optical Transfer Function: the OTF is equal to autocorrelation product through the pupil of (OMI) and (OM'I). The phase function P is due to the length difference of the optical paths.

This autocorrelation product reflects the phase delay due to light beam propagation, as well as the complex apodization function of the pupil.

Considering an apodization function $P(\vec{\rho})$, the OTF is expressed as

$$OTF_P(\vec{u}, \Psi) = \frac{1}{\pi} \int_0^{+\infty} \int_{-\pi}^{\pi} P\left(\vec{\rho} - \frac{\vec{u}}{2}\right) P^*\left(\vec{\rho} + \frac{\vec{u}}{2}\right) e^{j\Delta_M(\vec{\rho}-\frac{\vec{u}}{2})} e^{-j\Delta_M(\vec{\rho}+\frac{\vec{u}}{2})} \rho d\rho d\phi.$$

Thanks to Fresnel approximation, we can simplify this expression:

$$\begin{cases} \Delta_M\left(\vec{\rho} - \frac{\vec{u}}{2}\right) = \left(\frac{\pi L^2}{4\lambda} \frac{1}{d_l} + \Psi\right) \left(\left(\rho \cos(\phi) - \frac{u}{2} \cos(f_\phi)\right)^2 + \left(\rho \sin(\phi) - \frac{u}{2} \sin(f_\phi)\right)^2 \right) \\ \Delta_M\left(\vec{\rho} + \frac{\vec{u}}{2}\right) = \left(\frac{\pi L^2}{4\lambda} \frac{1}{d_l} + \Psi\right) \left(\left(\rho \cos(\phi) + \frac{u}{2} \cos(f_\phi)\right)^2 + \left(\rho \sin(\phi) + \frac{u}{2} \sin(f_\phi)\right)^2 \right) \end{cases}$$

Moreover, as we choose $f_\phi = 0$:

$$\begin{cases} \Delta_M\left(\vec{\rho} - \frac{\vec{u}}{2}\right) = \left(\rho^2 + \frac{u^2}{4} - u\rho \cos(\phi)\right) \left(\frac{\pi L^2}{4\lambda} \frac{1}{d_l} + \Psi\right) \\ \Delta_M\left(\vec{\rho} + \frac{\vec{u}}{2}\right) = \left(\rho^2 + \frac{u^2}{4} + u\rho \cos(\phi)\right) \left(\frac{\pi L^2}{4\lambda} \frac{1}{d_l} + \Psi\right) \end{cases}$$

Thus:

$$OTF_P(\vec{u}, \Psi) = \frac{1}{\pi} \int_0^{+\infty} \int_{-\pi}^{\pi} P\left(\vec{\rho} - \frac{\vec{u}}{2}\right) P^*\left(\vec{\rho} + \frac{\vec{u}}{2}\right) e^{j\left(-2u\rho \cos(\phi)\left(\frac{\pi L^2}{4\lambda} \frac{1}{d_l} + \Psi\right)\right)} \rho d\rho d\phi$$

We rewrite the phase function θ defined in (2) as:

$$\theta(\rho) = \frac{\pi L^2}{4d_l} \rho^2 + \theta'(\rho) \quad (7)$$

Then,

$$OTF_P(u, \Psi) = \frac{1}{\pi} \int_0^{+\infty} \int_{-\pi}^{\pi} \left| P\left(\vec{\rho} - \frac{\vec{u}}{2}\right) \right| \left| P^*\left(\vec{\rho} + \frac{\vec{u}}{2}\right) \right| e^{j\left(\theta'\left(\vec{\rho}-\frac{\vec{u}}{2}\right) - \theta'\left(\vec{\rho}+\frac{\vec{u}}{2}\right)\right)} e^{j2u\Psi\rho \cos(\phi)} \rho d\rho d\phi$$

In Eq. (7), the term $\frac{\pi L^2}{4d_l} \rho^2$ represents the delay introduced by a focal-infinity pair; the term $\theta'(\vec{\rho})$ represents the aberrations of the lens. Using the revolution symmetrical property of the pupil, we can write the OTF as

$$OTF_P(u, \Psi) = \frac{2}{\pi} \int_0^{+\infty} \int_0^{\pi} \left| P\left(\vec{\rho} - \frac{\vec{u}}{2}\right) \right| \left| P^*\left(\vec{\rho} + \frac{\vec{u}}{2}\right) \right| \cos\left(2u\Psi\rho \cos(\phi) + \left(\theta'\left(\vec{\rho} - \frac{\vec{u}}{2}\right) - \theta'\left(\vec{\rho} + \frac{\vec{u}}{2}\right)\right)\right) \rho d\rho d\phi. \quad (8)$$

Equation (8) represents the general expression of the OTF of any achromatic, revolution symmetrical optic. It allows an easy interpretation of WFC techniques. In fact, the objective of WFC is to maximize the OTF on the largest defocus zone. The maximal OTF is obtained by making the cosine in (8) equal to 1, which is equivalent to the following criterion:

$$2u\Psi\rho \cos(\phi) + \left(\theta'\left(\vec{\rho} - \frac{\vec{u}}{2}\right) - \theta'\left(\vec{\rho} + \frac{\vec{u}}{2}\right)\right) = 0 \quad \forall \vec{\rho}, \Psi \quad (9)$$

In other words, WFC consists on proposing a function mask θ' that fits the criterion (9). Fitting should be done on a range of frequencies u , and a range of focus Ψ , which is the image of the depth of field through the lens. Satisfying this criterion is obviously impossible, thus, the DOF is necessarily limited.

2.5.2 OTF of diffraction-limited systems

Equation (8) defines the OTF of any optic. It can be applied to the particular case of diffraction-limited systems. Such a system does not have aberrations ($\theta(\vec{\rho}) = \text{constant}$), and we suppose that its complex apodization is unitary, i.e $P(\vec{\rho}) = 1$ or 0.

Let us introduce the domain $Area(u)$ such that:

$$P\left(\vec{\rho} - \frac{\vec{u}}{2}\right)P^*\left(\vec{\rho} + \frac{\vec{u}}{2}\right) \begin{cases} \neq 0 & \text{if } \vec{\rho} \in Area(u) \\ 0 & \text{else} \end{cases}$$

The domain $Area(u)$ defines the integration domain for the diffraction's OTF:

$$OTF_{diff}(u, \Psi) = \frac{2}{\pi} \iint_{Area(u)} \cos(2u\Psi\rho \cos(\Phi)) \rho d\rho d\phi$$

We can now express the OTF with an average value:

$$OTF_{diff}(u, \Psi) = \frac{2}{\pi} Area(u) \overline{\cos(2u\Psi\rho \cos(\Phi))}_{Area(u)}$$

Considering that the average value $\overline{\cos(2u\Psi\rho \cos(\Phi))}_{Area(u)}$ is constant onto the pupil:

$$\overline{\cos(2u\Psi\rho \cos(\Phi))}_{Area(u)} \approx \overline{\cos(2u\Psi\rho \cos(\Phi))}_{on\ pupil} = \frac{2}{\pi} \int_0^1 \int_0^\pi e^{j2u\Psi\rho \cos(\Phi)} \rho d\rho d\phi.$$

Then

$$OTF_{diff}(u, \Psi) \approx \left(\frac{2}{\pi}\right)^2 Area(u) \cdot \overline{\cos(2u\Psi\rho \cos(\Phi))}_{on\ pupil}.$$

Using the known result⁸: $Area(u) = \left(\arccos\left(\frac{u}{2}\right) - \frac{\sqrt{u^2}}{2} \sqrt{1 - \left(\frac{u}{2}\right)^2} \right)$, we have

$$OTF_{diff}(u, \Psi) \approx \frac{2}{\pi} \left(\arccos\left(\frac{u}{2}\right) - \frac{u}{2} \sqrt{1 - \left(\frac{u}{2}\right)^2} \right) \left(\frac{2}{\pi} \int_0^1 \int_0^\pi \cos(2u\Psi\rho \cos(\Phi)) \rho d\rho d\phi \right),$$

$$OTF_{diff}(u, \Psi) = \frac{2}{\pi} \left(\arccos\left(\frac{u}{2}\right) - \frac{u}{2} \sqrt{1 - \left(\frac{u}{2}\right)^2} \right) \int_0^1 J_0(2u\Psi\rho) \rho d\rho.$$

This leads us to Smiths' known result¹⁴

$$OTF_{diff}(u, \Psi) = \frac{2}{\pi} \left(\arccos\left(\frac{u}{2}\right) - \frac{u}{2} \sqrt{1 - \left(\frac{u}{2}\right)^2} \right) \frac{J_1(2u\Psi)}{u\Psi} \quad (10)$$

Equation (10) is consistent with Goodmans' results⁸: when we focus an optical system at infinity, (i.e. $\Psi \rightarrow 0$), we find the OTF of a classical diffractive system.

$$\Psi \rightarrow 0 \quad OTF_{diff}(u, 0) \rightarrow \frac{2}{\pi} \left(\arccos\left(\frac{u}{2}\right) - \frac{u}{2} \sqrt{1 - \left(\frac{u}{2}\right)^2} \right)$$

2.6 Depth of field definition

The depth of field can be defined in different ways. In this paper, we use an OTF based definition: for a given frequency, the image (I) of an object (O) will be considered as sufficiently discernable if the modulus of the OTF at this frequency is greater than a given threshold. We denote by $DOF(u, b)$ the depth of field at frequency u for a detection threshold b , which is the greatest interval (Ψ_1, Ψ_2) such that for all Ψ in this interval, $OTF_p(u, \Psi) \geq b$.

If we now consider a bandwidth of spatial frequency of interest $(0, u_{max})$, the DOF at threshold b is

$$DOF(b) = \bigcap_{0 \leq u \leq u_{max}} DOF(u, b). \quad (11)$$

In other terms, the depth of field is the largest interval of focus such that the OTF remains above b for all frequencies between 0 and u_{max} .

3. ACHROMATIC REVOLUTION SYMMETRIC LIMIT (ARSL)

In the previous section, we introduced the notion of OTF of any optics, as well as the notion of DOF. We now consider the OTF limitation, which will subsequently limit the DOF.

3.1 OTF limitation

Equation (8) does not directly provide an a priori limit of the OTF for any apodization function $P(\vec{\rho})$. We consider instead an average value of the OTF upon a given range of defocus.

$$\begin{aligned}\overline{OTF_P(u)}_{\Psi_{lim}} &= \frac{2}{\pi\Psi_{lim}} \int_{-\frac{\Psi_{lim}}{2}}^{\frac{\Psi_{lim}}{2}} \int_0^{+\infty} \int_0^\pi \left| P\left(\vec{\rho} - \frac{\vec{u}}{2}\right) \right| \left| P^*\left(\vec{\rho} + \frac{\vec{u}}{2}\right) \right| \cos\left(2u\Psi_{lim}\cos(\phi) + \left(\theta'\left(\vec{\rho} - \frac{\vec{u}}{2}\right) - \theta'\left(\vec{\rho} + \frac{\vec{u}}{2}\right)\right)\right) \rho d\rho d\phi d\Psi \\ \overline{OTF_P(u)}_{\Psi_{lim}} &= \frac{2}{\pi} \int_0^{+\infty} \int_0^\pi \frac{\left| P\left(\vec{\rho} - \frac{\vec{u}}{2}\right) \right| \left| P^*\left(\vec{\rho} + \frac{\vec{u}}{2}\right) \right| \cos\left(\theta'\left(\vec{\rho} - \frac{\vec{u}}{2}\right) - \theta'\left(\vec{\rho} + \frac{\vec{u}}{2}\right)\right) \sin(2u\rho\Psi_{lim}\cos(\phi))}{2u\rho\Psi_{lim}\cos(\phi)} \rho d\rho d\phi\end{aligned}$$

We now want to find an upper bound of the average value of the OTF. Let us remark that taking $\theta' = 0$ in the previous expression is considering a lens only limited by diffraction. This leads to the following bound.

$$\overline{OTF_P(u)}_{\Psi_{lim}} \leq \frac{2}{\pi} \int_0^{+\infty} \int_0^\pi \left| \frac{\left| P\left(\vec{\rho} - \frac{\vec{u}}{2}\right) \right| \left| P^*\left(\vec{\rho} + \frac{\vec{u}}{2}\right) \right| \sin(2u\rho\Psi_{lim}\cos(\phi))}{2u\rho\Psi_{lim}\cos(\phi)} \right| \rho d\rho d\phi \quad (12)$$

This equation is one of the key results of this article. Therefore, it is worth an interpretation. The right hand term is the mean value of the absolute value of the OTF of diffraction. Therefore, for all phase functions, a given defocus and a given spatial frequency, the average of the OTF on the range of defocus is lower than the average of the OTF of diffraction. It does not mean that the OTF is lower than the diffraction OTF everywhere. The inequality is only an upper bound in average. This property is used by WFC lenses: the OTF is distributed along the defocus range as evenly as possible. The diffraction is optimal only in average, but it can be beaten when its values are low by trading some higher values of OTF.

Geometrically speaking the average OTF is related to the area below the curve of the through focus OTF (see Fig. 3). For any range of defocus, the area below the OTF curve of any WFC lens is lower than the area below the through focus diffraction OTF. The game of WFC design is to make this OTF higher than a given threshold and as even as possible for all frequencies.

Considering the definition of the domain $Area(u)$, we have the following comparison

$$\begin{aligned}\frac{2}{\pi} \int_0^{+\infty} \int_0^\pi \left| \frac{\left| P\left(\vec{\rho} - \frac{\vec{u}}{2}\right) \right| \left| P^*\left(\vec{\rho} + \frac{\vec{u}}{2}\right) \right| \sin(2u\rho\Psi_{lim}\cos(\phi))}{u\rho\Psi_{lim}\cos(\phi)} \right| \rho d\rho d\phi &\leq \frac{2}{\pi} \iint_{Area(u)} \left| \frac{\sin(2u\rho\Psi_{lim}\cos(\phi))}{2u\rho\Psi_{lim}\cos(\phi)} \right| \rho d\rho d\phi \\ \overline{OTF_P(u)}_{\Psi_{lim}} &\leq \frac{2}{\pi} \cdot \frac{Area(u)}{Area(u)} \iint_{Area(u)} \left| \frac{\sin(2u\rho\Psi_{lim}\cos(\phi))}{2u\rho\Psi_{lim}\cos(\phi)} \right| \rho d\rho d\phi\end{aligned}$$

A numerical study of the function $\Psi_{lim} \rightarrow \overline{|\sin c(2u\rho\Psi_{lim}\cos(\phi))|}_{Area(u)}$ shows that f is bounded from above by the function $\Psi_{lim} \rightarrow \overline{|\sin c(2u\rho\Psi_{lim}\cos(\phi))|}_{whole\ pupil}$.

This observation provides the following universal upper bound of the average value of any apodization function:

$$\overline{OTF_P(u)}_{\Psi_{lim}} \leq Area(u) \frac{2}{\pi} \left(\frac{2}{\pi} \int_0^1 \int_0^\pi \left| \frac{\sin(2u\rho\Psi_{lim}\cos(\phi))}{2u\rho\Psi_{lim}\cos(\phi)} \right| \rho d\rho d\phi \right)$$

3.2 ARSL Theorem

We now come to the main result of this paper. For any achromatic, revolution symmetric optic, average OTF on axis is necessarily limited by a function called the achromatic revolution symmetric limit (ARSL):

$$ARSL(u, \Psi_{lim}) = \frac{4}{\pi^2} \left(\arccos\left(\frac{u}{2}\right) - \frac{u}{2} \sqrt{1 - \left(\frac{u}{2}\right)^2} \right) \int_0^1 \int_0^\pi |\text{sinc}(2u\rho\Psi_{lim} \cos(\phi))| \rho \, d\rho d\phi \quad (13)$$

$$\forall P(\rho) \overline{OTF_p(u)_{\Psi_{lim}}} \leq ARSL(u, \Psi_{lim}) \quad (14)$$

Furthermore, when $\Psi_{lim} \rightarrow 0$ (which means that the object is set at infinity, $d_o \rightarrow \infty$), this limit boils down to the limit of the OTF of a diffractive system: $\overline{OTF_p(u)_{\Psi_{lim}}} \rightarrow \frac{2}{\pi} \left(\arccos\left(\frac{u}{2}\right) - \frac{u}{2} \sqrt{1 - \left(\frac{u}{2}\right)^2} \right)$. It only means that very locally around the position of best focus, the optimal blur is given by the diffraction.

3.3 Physical interpretation of ARSL

As previously explained, the ARSL is not a point wise limitation of the OTF. It is an upper bound of the average value of the OTF. Consequently, it provides an upper bound of the area beyond the plot of OTF. This obviously limits the magnitude of the optimal OTF. Let us consider the following example.

Given a range of defocus, the best OTF is constant over this range (i.e for all $|\Psi| < \frac{\Psi_{lim}}{2}$), and null elsewhere.

In Figure 3, we consider a frequency $u=0.4$, and $\Psi_{lim}=17$. According to the ARSL theorem, the OTF could be expressed as follows:

$$BestOTF = \begin{cases} ARSL(u = 0.4, \Psi) = 0.3 & \text{if } |2\Psi| < 17 \\ 0 & \text{else} \end{cases}$$

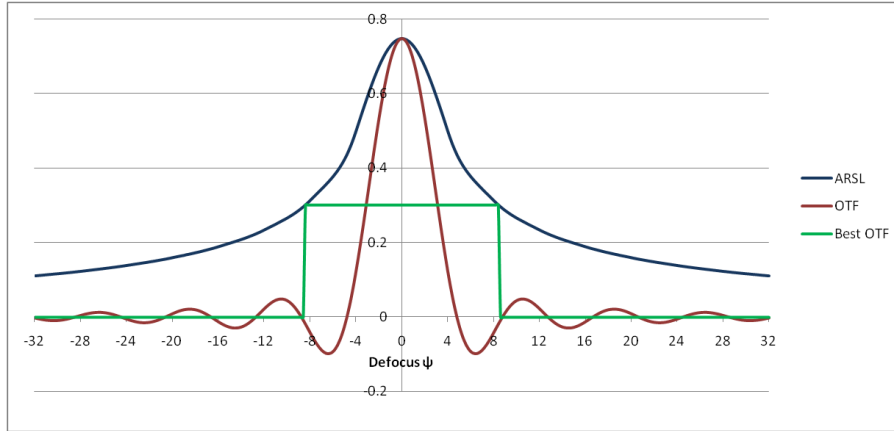


Figure 3 ARSL and diffraction OTF versus defocus parameter ψ

3.4 Comparison with diffraction

The main advantage of EDOF techniques is to extend the depth of field of a common optic. In order to appreciate the gain of WFC techniques, it is interesting to compare the ARSL behavior with a classical diffractive system.

For small values of $u\Psi_{lim}$, we have $\text{sinc}(u\rho\Psi_{lim} \cos(\phi)) > 0$, therefore

$$\overline{OTF_p(u)_{\Psi_{lim}}} \leq \frac{2}{\pi} \int_0^{+\infty} \int_0^\pi \left| \frac{P\left(\vec{\rho} - \frac{\vec{u}}{2}\right) \left| P^*\left(\vec{\rho} + \frac{\vec{u}}{2}\right) \sin(2u\rho\Psi_{lim} \cos(\phi)) \right|}{2u\rho\Psi_{lim} \cos(\phi)} \right| \rho d\rho d\phi$$

$$\overline{OTF_P(u)}_{\Psi_{lim}} \leq \frac{2}{\pi\Psi_{lim}} \int_{-\frac{\Psi_{lim}}{2}}^{\frac{\Psi_{lim}}{2}} \int_0^{+\infty} \int_0^{\pi} \left| P\left(\rho - \frac{u}{2}\right) \right| \left| P^*\left(\rho + \frac{u}{2}\right) \right| \cos(2u\Psi\rho \cos(\Phi)) \rho d\rho d\phi d\Psi$$

$$\overline{OTF_P(u)}_{\Psi_{lim}} \leq \frac{1}{\Psi_{lim}} \int_{-\frac{\Psi_{lim}}{2}}^{\frac{\Psi_{lim}}{2}} \frac{2}{\pi} \left(\arccos\left(\frac{u}{2}\right) - \frac{u}{2} \sqrt{1 - \left(\frac{u}{2}\right)^2} \right) \frac{J_1(2u\Psi)}{u\Psi} d\Psi$$

$$\overline{OTF_P(u)}_{\Psi_{lim}} \leq \overline{OTF_{diff}(u)}_{\Psi_{lim}}$$

For small values of $u\Psi_{lim}$, the ARSL consists in distributing the area under the plot of diffraction function. This observation reinforces the idea that WFC techniques mainly aim to “spread the diffractive OTF”.

3.5 ARSL behavior versus frequency

Formula (12) expresses the ARSL as a function of frequency. In figure 5, the ARSL is plotted for different frequency values u . These ARSL are obviously decreasing with respect to frequency.

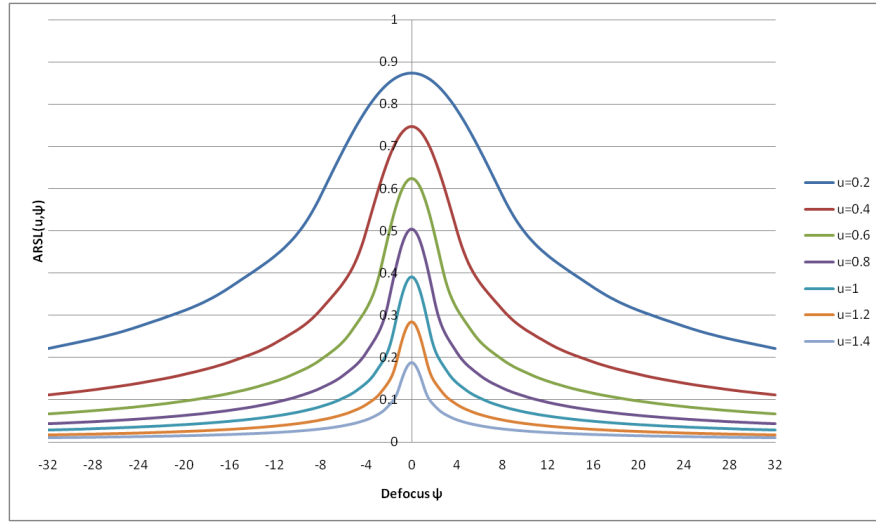


Figure 3 ARSL for different normalized frequencies: the DOF decreases with the frequency.

3.6 ARSL Theorem consequence

According to DOF definition (11), the DOF is determined by the maximum frequency chosen by the user.

$$DOF_{ARSL}(b) = DOF(u_{max}, b) \quad (15)$$

As the ARSL is a decreasing function of defocus, the extension of depth of field yield by a WFC technique can only be done by a loss of OTF gain. A trade-off has to be done between the possible DOF and the OTF level. For large defocus value, this trade-off could be expressed as follows:

$$\Psi_{lim} ARSL(u, \Psi_{lim}) \approx cst(u)$$

$$ARSL(u, \Psi) = \frac{cst(u)}{\sqrt{\Psi}}$$

4. ARSL APPLICATION ON A NUMERICAL EXAMPLE

In the previous sections, we proved that the performances of any achromatic revolution symmetric optic are necessary limited. Let us try to find out if this limit is realistic, using the characteristics of a common camera module for camera phones:

- Lens for camera phone of 5MPx
- Pixels of size $\alpha = 1.75\mu m$: the Nyquist's frequency is given by $F_{Nyq} = \frac{1}{2 \cdot 1.75\mu m} \approx 285 \text{ lp/mm}$.
- The aperture is characterized by $N = 2.4$
- The sensor is placed in $d_I \approx f'$: $\Psi = \frac{\pi L^2}{4 \lambda d_o}$.
- $\sin \alpha' \approx \frac{1}{2N}$ and if $d_o \gg f'$: $f' : f' = L \sqrt{N^2 - \frac{1}{4}} \approx NL = 3.26 \text{ mm}$ (true under Fresnel's approximation)
- Optimal normalized frequency (Nyquist/2): $u_{max} = \frac{\frac{\lambda d_I F_{Nyq}}{2}}{\frac{L}{2}} = \frac{\lambda f' F_{Nyq}}{L} \approx \lambda N F_{Nyq} \approx \frac{\lambda N}{a} \approx 0.34$.
- The wavelength is $\lambda = 486 \text{ nm}$.

4.1 How to determine the best DOF from the ARSL?

The DOF is defined for maximal frequency u_{max} and a threshold of detection b . The threshold b fixes a limiting Ψ_{min} such as $ARSL(u_{max}, \Psi_{min}) = b$

Thus, the lower bound of the DOF, also called the minimal object distance (MOD) is given by:

$$d_{0min} = \frac{\pi f'^2}{4N^2 \lambda \Psi_{min}}$$

The DOF is the interval $(d_{0min}, +\infty)$.

In the present example, we set the detection threshold $b = 0.4$. Thus, the best possible OTF constant at 40% upon the DOF range gives $\Psi_{min} = 13.6$ and the DOF is 21cm to infinity. Figure 6 shows the ARSL plot versus defocus, for maximum available frequency $u_{max} = 0.34$.

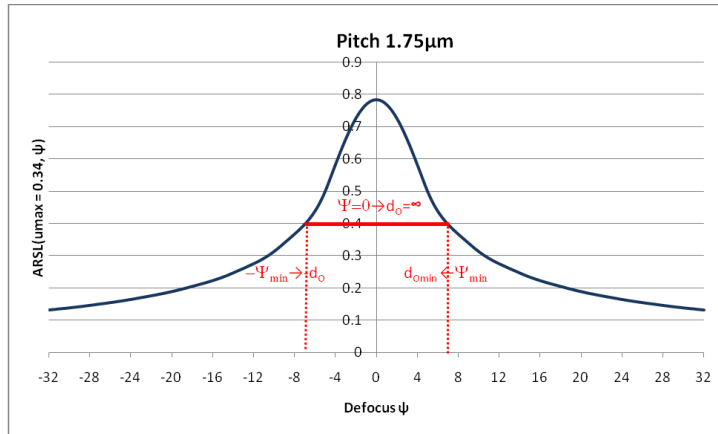


Figure 4 ARSL for $u_{max} = 0.34$ versus defocus Ψ_{lim}

Obviously, the DOF value is closely dependent on the fixed threshold. Thus, best benefits from WFC techniques come with low threshold values, which correspond to a better handling of low SNR.

4.2 DOF Limitation with the pixels size reduction

Nowadays, camera resolution is increasing, and pixel size is decreasing. Let us see what happens with ARSL. In Figure 7, we plot the ARSL and the OTF of diffraction for pixel pitches from $1.75\mu m$ to $1.1\mu m$, with a constant field of view.

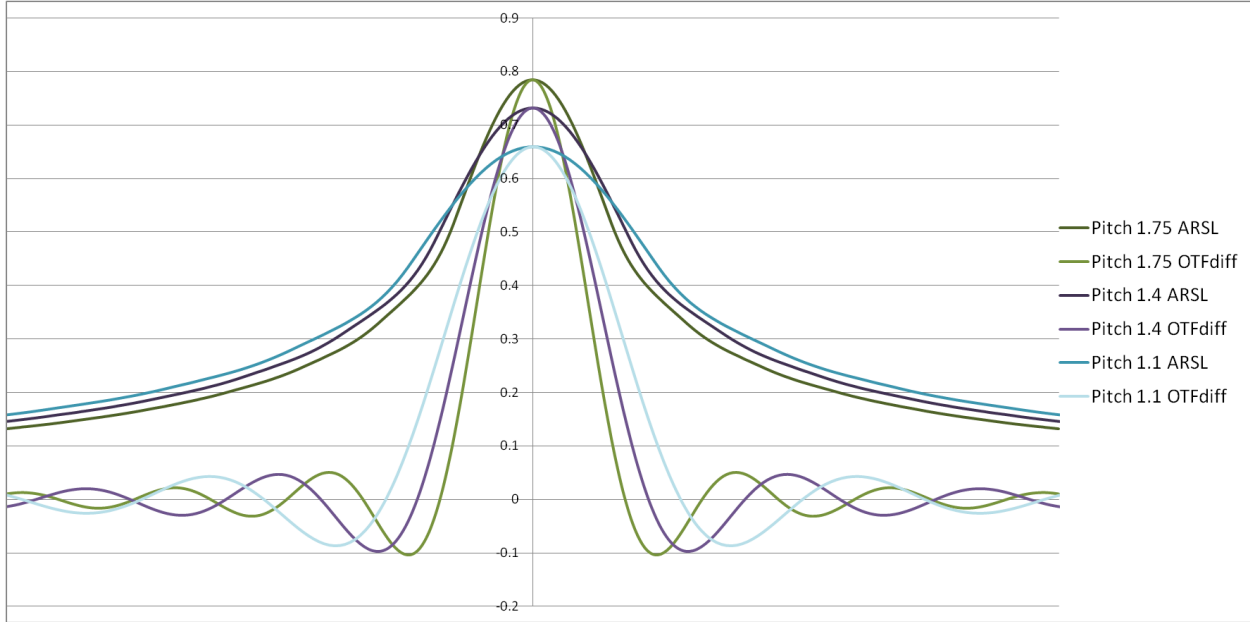


Figure 5 ARSL and OTF of diffraction for different pixel pitches

Table 1 represents the DOF associated with each pixel pitch.

Table 1. DOF evolution with pixel pitch.

Pitch (μm)	1.75	1.4	1.1
Detection threshold b	40%		
ARSL defocus ψ_{\min}	13.9	15.46	16.9
ARSL DOF	21cm to infinity	19cm to infinity	18cm to infinity
Diffraction defocus ψ_{\min}	6.3	7.7	9.12
Diffraction DOF	46cm to infinity	38cm to infinity	32cm to infinity
MOD_{ARSL}/MOD_{diff}	2.2	2.0	1.8

It appears that the DOF grows larger when the pixel pitch gets smaller. In fact, the diffraction spot becomes very large compared to the sensor dimensions as the pixel pitch decreases. However, the DOF gain obtained by a WFC lens compared to a classical diffractive system decreases, meaning that the advantage of WFC with regards to the diffraction is also reduced.

5. CONCLUSION

In this article, we introduced the ARSL (Achromatic Revolution Symmetric Limit) which determines an upper bound to the depth of field of a lens using a wavefront coding technique. The ARSL does not provide the optimal lens design explicitly but it quantifies the tradeoff between the level of the OTF and the depth of field. An important point is that diffraction naturally operates a similar effect to the aberration introduced by the lens. Therefore, when the pixel pitch becomes smaller, the extension of depth of field becomes more and more marginal when compared with a normal lens. Let us also remark that the ARSL is a very optimistic bound, since it is only computed at the image center and for a

single wavelength. It does not account for unpredictable variations in mass production or loss due to the sensor. A possibility to further extend the depth of field is to use other type of methods which are independent from diffraction, for instance methods based on longitudinal chromatic aberration.

REFERENCES

- [1] Cathey, W. T., Dowski, E., "A new paradigm for imaging systems", *Applied Optics* 41 , 6080–6092 (2002).
- [2] Chi, W., George, N., "Electronic imaging using a logarithmic asphere", *OPTICS LETTERS*, Vol. 26, No. 1 (2001).
- [3] Dowski, E. R., Johnson, G. E. (1999). "Wavefront coding: a modern method of achieving high-performance and/or low cost imaging systems," *Current Developments in Optical Design and Optical Engineering VIII*, Proc. SPIE Vol.3779 (pp. 137-145). San Francisco: Robert E. Fischer; Warren J. Smith.
- [4] Dowski, E., Cathey, W. , "Extended depth of field through wave-front coding", *J. of Applied Optics (OSA)* 34(11) , 1859-1866 (1995).
- [5] Dowski, E., Cormack, R.H., Samara, S.D., "Wavefront Coding: jointly optimized optical and digital imaging systems," *Proc SPIE Int. Soc. Opt.* (2000)
- [6] Fales, C. L., Huck, F. O., Samms, R. W., "Imaging system design for improved information capacity," *Appl. Opt.* 23 , 872-888 (1984).
- [7] Goodman, J., "Statistical Optic," New York: Wiley (1985).
- [8] Goodman, J. W., "Introduction to Fourier Optics," New York: McGraw-Hill (1986).
- [9] Guichard, F., Cao, F., Tisse, C., "Image processing challenges in a world of small pixels," *Proc. Of the IntertechPira, Images Sensors Conference in London, UK* (2008).
- [10] Lépine, J. A., "Bases de Radiométrie Optique," Cêpaduès Editions (2001).
- [11] Linfoot, E. H., "Information Theory and Optical Images," *J. Opt. Soc. Am.* 45 , 808-818 (1955).
- [12] Raveh, I., Zalevsky, Z., "All-optical axially multi-regional super resolved imaging," *Optics Express (OSA)* 15(26) , 17912-17921 (2007).
- [13] Shannon, C., "A mathematical theory of communication," *The Bell System Technical Journal* 27 , 623-656 (1948).
- [14] Smith, W. J., "Modern Optical Engineering," New York: McGraw-Hill (2000).
- [15] Tisse, C., Guichard, F., Cao, F., "Does resolution really increase image quality?," *Proc. of SPIE Conference on Electronic Imaging: Digital Photography IV*, (p. 6817). San Francisco (2008).
- [16] Tisse, C.-L., Nguyen, H. P., Tessières, R., Pyanet, M., Guichard, F., "Extended depth-of-field (EDoF) using sharpness transport across color channels," *Proc. of SPIE Conference on Optics Photonics: Optical Engineering + Applications, Novel Optical Systems Design and Optimization XI*. San Francisco (2008).
- [17] van der Gracht, J., Nagy, J. G., Paul Pauca, V., Plemmons, R. J., "Iterative Restoration of Wavefront Coded Imagery for Focus Invariance," *Optical Society of America (OSA)* (2001) .
- [18] Wang, H., Gan, F., "High focal depth with a pure-phase apodizer," *APPLIED OPTICS* Vol. 40, No. 31 (2001).
- [19] Zalevsky, Z., Shemer, A., Zlotnik, A., Eliezer, E., Marom, E., "All-optical axial super resolving imaging using a low-frequency binary-phase mask," *Optics Express (OSA)* 14(7) , 2631-2643 (2006).